Pergamon

Geochimica et Cosmochimica Acta, Vol. 65, No. 15, pp. 2605–2614, 2001
Copyright © 2001 Elsevier Science Ltd
Printed in the USA. All rights reserved
0016-7037/−1899 $20.00 + .00

PII S0016-7037(01)00605-6

Correction for volatile fractionation in ascending magmas: Noble gas abundances in primary mantle melts

PETE BURNARD*

Division of Geological and Planetary Sciences, California Institute of Technology MS100-23, Pasadena CA 91125, USA

(*Received November* 28, 2000; *accepted in revised form February* 12, 2001)

Abstract—Accurate relative noble gas abundances of mantle-derived melts are required in order to further understand the distribution of noble gases in the mantle and fractionation of noble gases during the melting process. Noble gas relative abundances in the majority of oceanic basalts are highly fractionated, at least in part due to late stage, solubility controlled fractionation. Noble gas concentrations in the volatile phase (≡ noble gas:CO_2 ratio) will vary systematically during solubility controlled degassing of a magma. This contribution models the noble gas concentrations in the volatile phase during degassing at different pressures and vesicularities in order to develop a method for correcting fractionation resulting from magmatic degassing, and thereby estimate the "initial" (pre-degassing) noble gas compositions.

Correcting for fractionation during magmatic degassing requires: a) a method for determining the volatile fractionation trajectory during degassing; and b) one well constrained mantle volatile composition with which to "fix" the extrapolation.

The trajectory of volatile fractionation can be estimated by sequential crushing of basaltic glasses. Vesicles grow during ascent, therefore large vesicles trap early (less fractionated) volatiles while small vesicles trap late (fractionated) volatiles. Sequential crushing of basaltic glasses releases volatiles from progressively smaller vesicles, thereby allowing the fractionation trajectory resulting from degassing to be determined on individual samples.

The production rate of both ^{21}Ne and ^{4}He in the mantle is a function of U concentration only, resulting in a constant $^{21}Ne/^{4}He$ production ratio in the mantle which can be used to "fix" the degassing fractionation trajectory determined by sequential crushing. This correction then allows fractionation of ^{4}He from ^{40}Ar *prior* to degassing to be assessed. This method is illustrated using multiple crushes of a single basaltic glass from the mid-Atlantic Ridge that shows that ^{4}He appears to have been fractionated from ^{40}Ar before degassing. *Copyright © 2001 Elsevier Science Ltd*

1. INTRODUCTION

Noble gas geochemistry is an essential tool for determining how the Earth's mantle has evolved in space and time. The abundances of noble gases in the solid Earth are low and consequently their isotopic composition is susceptible to modification by radiogenic or nucleogenic "clocks." Also, the noble gases are inert at geological pressures and temperatures; and this combination of inertness and volatility makes them particularly useful as tracers for the major volatile species in the mantle, water, and CO_2.

Previous studies of He, Ne, Ar, and Xe in mantle derived samples have established the first order noble gas *isotopic* variations of the mantle. The mantle can be subdivided into a well mixed region with high $U/^{3}He$ as sampled by midocean ridge basalts (MORBs), and a heterogeneous region characterized by less radiogenic He (lower time-integrated $U/^{3}He$), sampled by ocean island basalts (OIBs). The OIB source region is thought to represent less processed material with higher ^{3}He concentrations due to preservation of a larger proportion of its primordial volatiles (e.g., Allègre et al., 1986; Allègre et al., 1983; Kurz and Jenkins, 1981). More recently, models have proposed that primordial noble gases (i.e., ^{3}He, ^{20}Ne, ^{22}Ne, and ^{36}Ar) in the MORB source region were not trapped there during accretion, but originated in the less degassed portion of the mantle and are "in transit" through the degassed mantle (thought to be the upper mantle) (Kellogg and Wasserburg, 1990; O'Nions and Tolstikhin, 1994; Porcelli and Wasserburg, 1995). Thus the isotopic composition of noble gases in the upper mantle result from primordial noble gases that originated in less degassed parts of the mantle and radiogenic noble gases that were produced in situ during an upper mantle residence time of ≈ 1 Ga.

While noble gas isotopic variations in the mantle are comparatively well established, the *relative* noble gas compositions of the mantle are difficult to constrain, due to numerous processes that can fractionate one noble gas from another. In spite of these difficulties, there is an increasing need for reliable relative noble gas compositions. It is difficult to test models of mantle—atmosphere noble gas evolution without relative noble gas data (Harrison et al., 1999), and valuable information on the time integrated K-U-Th systematics of the mantle can be obtained from their decay products, ^{4}He, ^{21}Ne, and ^{40}Ar. However, estimating the relative noble gas compositions in the mantle is not straightforward as noble gases are likely to fractionate from each other during transport of the magma from the melting zone to the surface. Indeed, the majority of basaltic glasses preserve a range in noble gas relative compositions within a single sample that likely reflect different stages of volatile evolution during the magma's history (Burnard, 1999; Fisher, 1997; Jambon et al., 1985; Marty et al., 1983; Marty and Ozima, 1986).

*Author to whom correspondence should be addressed (peteb@gps.caltech.edu)

The residual concentration of mantle volatiles (including noble gases) in a rock are often determined by secondary processes, a reflection of the eruption history or vesicle (or fluid inclusion) distribution, rather than the primary concentration in the mantle. To a great extent, the effects of these secondary processes can be circumvented by directly determining noble gas concentrations within the volatile phase (Burnard, 1999; Marty and Zimmerman, 1999). In most oceanic basalts volatiles are dominated by CO_2, therefore the noble gas concentration in the volatile phase is equivalent to the noble gas:CO_2 ratio (Burnard, 1999; Marty and Zimmerman, 1999). Noble gas concentrations in the volatile phase are not subject to variations in vesicle or inclusion density, but vary systematically depending on the extent and mechanism of gas loss from the magma. This contribution explores how magmatic volatile processes will affect the noble gas concentrations in the volatile phase and how these can be measured. The primary goal of this work is to demonstrate that it is possible to correct for volatile fractionation during gas loss; however, the lack of a large combined He-Ne-Ar-CO_2 database for oceanic basalts precludes a retrospective analysis of degassing in oceanic basalts. Analysis of a single sample demonstrates that stepwise crush analyses of He, Ne, Ar, and CO_2 permits correction for late stage magmatic degassing. The ability to deconvolve degassing fractionation is necessary to estimate relative noble gas abundances of primary mantle melts.

2. VOLATILES IN OCEANIC BASALTS

2.1. Initial Compositions

The composition of volatiles in a primary mantle melt—i.e., their composition before any gas loss—is not well known. Variations in the "initial" (i.e., predegassing) melt volatile composition may arise from compositional differences in the mantle or from fractionation during melting of the mantle.

Some constraint on the "initial" volatile compositions can be gained from the radiogenic or nucleogenic noble gas isotopes, ^{4}He, ^{21}Ne, and ^{40}Ar, which are produced by lithophile elements in the mantle. It is possible to estimate their production ratios in the mantle from knowledge of lithophile element ratios. The radiogenic/nucleogenic noble gases can be corrected for addition of atmospheric noble gases, and are therefore ideal for studying magmatic volatile behavior (Jambon, 1994). Isotopes corrected for atmospheric addition are indicated by "*". ^{40}Ar* is calculated by assuming that all ^{36}Ar is derived from the atmosphere: the ^{40}Ar/^{36}Ar ratio of the MORB mantle ($\geq$40000; (Burnard et al., 1997; Moreira et al., 1998)) is sufficiently high that all ^{36}Ar measured in a sample can be assumed to be atmospheric in origin (^{40}Ar/^{36}Ar of air = 295.5). Calculating ^{21}Ne* requires that the mantle ^{21}Ne/^{22}Ne ratio is known, because a significant proportion of the non-nucleogenic isotope, ^{22}Ne, in a given analysis will not be atmospheric but will originate from the mantle. Uncertainties in the true ^{20}Ne/^{22}Ne ratio of the mantle results in uncertainty in the proportion of mantle-derived ^{21}Ne (Trieloff et al., 2000); the ^{21}Ne/^{22}Ne ratio of the mantle at a given ^{20}Ne/^{22}Ne ratio is well constrained for *N*-MORBs. For example, if the MORB-source ^{20}Ne/^{22}Ne = 13.8, then MORB ^{21}Ne/^{22}Ne = 0.074, whereas if (^{20}Ne/^{22}Ne)$_{MORB}$ = 12.5, then (^{21}Ne/^{22}Ne)$_{MORB}$ = 0.059 (Moreira et al., 1998; Sarda et al., 1988). In the worst instance, it is possible to perform a consistent correction for atmospheric derived Ne based on an assumed ^{20}Ne/^{22}Ne for the mantle. Atmospheric contamination is rarely a problem for He due to the low concentration of He in the atmosphere.

The ^{4}He/^{40}Ar ratio in a region of mantle is a function of time (as well as of mantle chemistry) because of differences in the U, Th, and K half-lives. Using reasonable estimates of mantle Th/U and K/U ratios (2.5 and 12700, respectively; (Jochum et al., 1983; O'Nions and McKenzie, 1995)), the instantaneous ^{4}He/^{40}Ar production ratio is $\approx$5, but this reduces to $\approx$1.5 if the radiogenic gases accumulate for $>$4.0 Ga (Allègre et al., 1986; Burnard et al., 1998; Ozima and Podosek, 1983). Reasonable estimates for the MORB source region ^{4}He/^{40}Ar are in the range 2 to 3, taking the likely mixing timescales of the upper mantle into account (Burnard et al., 1998; Marty and Zimmerman, 1999).

^{21}Ne is produced in the mantle by n,α and α,n reactions on ^{24}Mg and ^{18}O, respectively. O and Mg are evenly distributed in the mantle, therefore both ^{21}Ne and ^{4}He production are determined by the mantle U and Th abundances: as a result the production ratio, ^{21}Ne/^{4}He, *is constant irrespective of chemistry or accumulation time* (once secular equilibrium has been reached). The theoretical estimate for the ^{21}Ne/^{4}He production ratio is 4.5×10^{-8} (Yatsevich and Honda, 1997), which is in reasonable agreement with nucleogenic Ne found in crustal fluids (Ballentine, 1997; Drescher et al., 1998; Kennedy et al., 1990; Yatsevich and Honda, 1997). Only recent He – Ne fractionation will change this ratio: noble gas fractionation in the mantle will be erased by production of ^{21}Ne and ^{4}He in less than several hundred Ma.

Thus, the ^{21}Ne/^{4}He ratio of the mantle is likely to be constant and can be used to correct correlated variations in volatile tracers in a similar manner to petrologists correcting for magmatic differentiation by assuming a mantle MgO content of 8% (Klein and Langmuir, 1987). In contrast, changes in ^{4}He/^{40}Ar in the mantle may result from temporal and/or chemical differences in the mantle source region.

2.2. He and Ar in MORBs

Solubility considerations predict the He/Ar ratio of a basaltic melt will increase when gas is lost from that melt. The ^{4}He/^{40}Ar* ratios measured in MORB glasses are generally higher than the production/accumulation ratio, typically in the range 5 to 80 (e.g., Fisher, 1975; Fisher, 1997; Hilton et al., 1993; Hiyagon et al., 1992; Honda and Patterson, 1999; Jambon et al., 1985; Staudacher et al., 1989). Magmatic degassing was long thought to be the reason for high He/Ar ratios in oceanic basalts (Jambon et al., 1985). However, two recent findings have challenged this explanation:

1. Matsuda and Marty (1995) and Honda and Patterson (1999) showed that, with the notable exception of the high He concentrations in "popping rock," high ^{4}He/^{40}Ar* ratios occur in basaltic glasses that have *high* He contents, and
2. Fisher (1997) showed that the maximum ^{4}He/^{40}Ar* ratio of a sample broadly correlates with depth of eruption such that basalts erupted at greater depth have higher ^{4}He/^{40}Ar* than shallow—erupted basalts.

These observations are not consistent with magmatic degas-

sing as the primary control on $^4He/^{40}Ar^*$, which would predict high $^4He/^{40}Ar^*$ ratios in the most degassed basalts, viz. those with low He contents and/or those erupted at shallow depths (because the degree of degassing varies inversely with depth of eruption (Fisher, 1997; Moore, 1979)). Therefore, although solubility-determined degassing does occur in basaltic glasses (Burnard, 1999), it appears that this is not the primary control on He/Ar ratio trapped in basaltic glasses.

The range in He/Ar ratios of MORBs has instead been attributed to high He diffusivities relative to Ar. In one model, He (but not Ar) preferentially diffuses out of mantle minerals into melt pockets, resulting in high magmatic He/Ar ratios associated with high He abundances (Fisher, 1975; Fisher, 1997; Matsuda and Marty, 1995). In a second model, He and Ar are not fractionated from the mantle source ratio in primary mantle melts, but, as the magma crystallizes, Ar is trapped in crystallizing phases, whereas He diffuses out of crystals back into the melt. As a consequence, He/Ar and He content increase with magmatic differentiation (Honda and Patterson, 1999). While radiogenic He, Ne, and Ar are likely produced in the mantle with ratios at or close to the theoretical production ratios, these studies show that it does not automatically follow that primary magmatic melts will inherit noble gases with the same ratios. Whichever process is involved, it is first necessary to deconvolve the late-stage magmatic degassing "overprint" on the primary control on He/Ar ratio.

2.3. Implications of Preferential Noble Gas Extraction During Mantle Melting

The data available at present appear to be compatible with either of the above scenarios. The process of noble gas extraction from the mantle—fundamental to the evolution of noble gas isotopes—is poorly constrained despite three decades of studying mantle noble gases. An important consequence of this is that preferential extraction of He from the mantle—as proposed in the above mechanisms—will result in a decrease in the mantle He/Ar ratio over time.

OIB basalts are known to have lower He contents than MORBs, surprising considering OIBs are thought to originate in a region of mantle with high $^3He/U$ (Anderson, 1998; Matsuda and Marty, 1995; Marty and Tolstikhin, 1998). Independent degassing tracers (such as noble gas relative abundances) are inconsistent with significant gas loss from the Loihi parental magma (Moreira and Sarda, 2000, although see also Hilton et al., 1997) and He-Sr or He-Pb mixing systematics from several ocean islands are consistent with approximately equal concentrations of He in MORB and OIB magmas (Farley et al., 1992; Graham et al., 1996). Late stage magmatic degassing fails to account for the low abundances of ^3He in OIBs.

Alternatively, it is possible that the low He content of OIBs is related to the melting process and that decompression melting during MORB genesis results in preferential extraction of He from the mantle. Note that if this scenario persisted for a significant time—timescales of the order of mantle turnover ($\approx$ 1 Ga)—the result would be a higher $^3He/U$, and therefore higher $^3He/^4He$, in the OIB reservoir in comparison to the MORB reservoir. It is possible that He isotopic heterogeneities in the mantle result from the differences in melting styles during OIB and MORB genesis. However, before investigating differential extraction of He from the mantle, it is first necessary to be able to confidently correct for magmatic degassing in both tectonic environments.

2.4. Volatile Distillation During Gas Loss

Most, if not all, MORB basalts are supersaturated with respect to CO_2 at their eruption pressures, resulting in two phase (melt + CO_2 vapor) magmas. The noble gases will partition into the CO_2 bubbles. If the noble gases remain in equilibrium with the bubbles, the maximum fractionation between two noble gases for each stage of vesiculation tends to the ratio of their solubilities (Jambon et al., 1986; Marty and Zimmerman, 1999):

$$\frac{(C_l/C_j)}{(C_l/C_j)_o} = \frac{S_i}{S_j}$$

(Where C_i, C_j refer to the concentrations of i and j in the magma and S_i and S_j are the solubilities of i and j, respectively.) However, the observation that $^4He/^{40}Ar^*$ in MORB glasses commonly exceeds 50, and $S_{He}/S_{Ar} \approx 10$ in tholeiitic magmas, suggests that the noble gases do not remain in equilibrium with the bubbles, but a distillation mechanism operates (Marty and Zimmerman, 1999).

The concentrations of any pair of volatile species i and j in a magma undergoing distillation will depend on the fraction of volatiles lost from the system and their relative solubilities:

$$\frac{C_i}{C_j} = \left(\frac{C_i}{C_j}\right)_o F_i^{(1-\alpha_{i,j})} \quad (1)$$

F_i is the fraction of gas i that has been lost, $\alpha_{i,j}$ is the solubility ratio (S_i/S_j) and subscript 'o' refers to the initial composition before any gas loss occurred.

Normalizing to CO_2 results in three parallel equations, where $j = CO_2$ and $i =$ either ^4He, $^{21}Ne^*$ or $^{40}Ar^*$. Re-arranging these to eliminate "F" results in two simultaneous expressions (see Burnard, 1999, for full derivation):

$$\ln\left(\frac{^{40}Ar^*}{CO_2}\right) = \frac{(1-\alpha_{Ar,CO_2})}{(1-\alpha_{Ne,CO_2})}\left[\ln\left(\frac{^{21}Ne^*}{CO_2}\right) - \ln\left(\frac{^{21}Ne^*}{CO_2}\right)_o\right] + \ln\left(\frac{^{40}Ar^*}{CO_2}\right)_o \quad (2)$$

$$\ln\left(\frac{^{4}He}{CO_2}\right) = \frac{(1-\alpha_{He,CO_2})}{(1-\alpha_{Ne,CO_2})}\left[\ln\left(\frac{^{21}Ne^*}{CO_2}\right) - \ln\left(\frac{^{21}Ne^*}{CO_2}\right)_o\right] + \ln\left(\frac{He}{CO_2}\right)_o \quad (3)$$

In the mantle, $^{21}Ne^*/^4He$ must be at the production ratio, r, $\approx 4.5 \times 10^{-8}$. This allows $(^{21}Ne^*/CO_2)_o$ to be substituted by $[r\mathrm{X}(^4He/CO_2)_o]$ and Eqn. 3 can be reduced to:

$$\ln\left(\frac{^{4}He}{CO_2}\right) = m_{He,Ne}\ln\left(\frac{^{21}Ne^*}{CO_2}\right) + \left[-m_{He,Ne}\ln\left(r\,\frac{^{4}He}{CO_2}\right)_o + \ln\left(\frac{^{4}He}{CO_2}\right)_o\right] \quad (4)$$

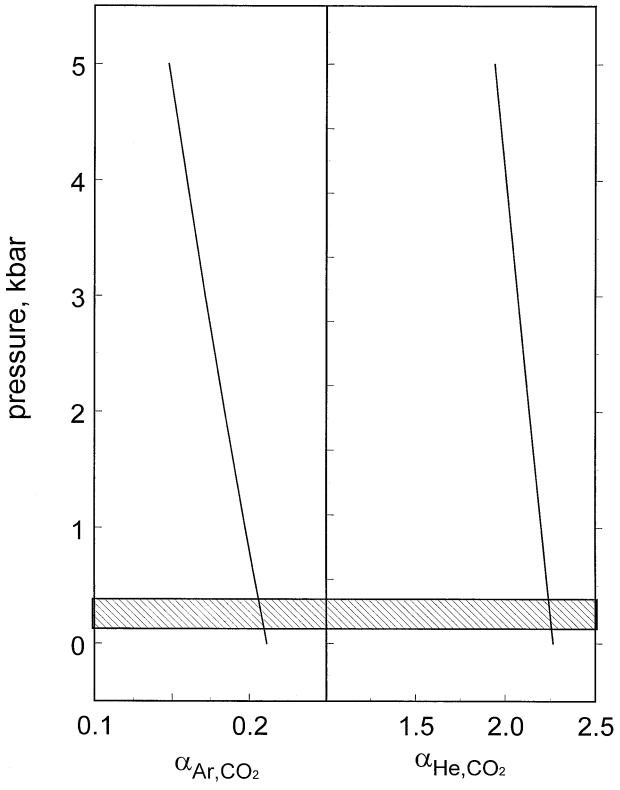

Fig. 1. Pressure dependence of α_{He,CO_2} and α_{Ar,CO_2} in the range 0 to 5 kbar assuming constant temperature and basalt composition. Shaded area indicates likely MORB eruption pressures. CO_2 solubilities are assumed to obey Henrian behavior in this pressure range; $Kh_{CO_2} = 9.32 \times 10^{-9}$ mol g^{-1} bar^{-1} (calculated for tholeiitic basalt according to Dixon 1997). Noble gas solubilities calculated from ionic porosities for tholeiitic basalt (Appendix; Carroll and Webster 1994).

Therefore, there will be a linear relation between $\ln(^4He/CO_2)$ and $\ln(^{21}Ne^*/CO_2)$ in the residual volatiles in a degassing magma. The slope, $m_{He,Ne} = (1 - \alpha_{He,CO_2})/(1 - \alpha_{Ne,CO_2})$ is a function only of the relative solubilities while the initial $^4He/CO_2$ and $^{21}Ne/CO_2$ compositions, $(^4He/CO_2)_o$ and $(^{21}Ne^*/CO_2)_o$, can be estimated from the intercept. Similarly for Ar:

$$\ln\left(\frac{^{40}Ar}{CO_2}\right) = m_{Ar,Ne} \ln\left(\frac{^{21}Ne^*}{CO_2}\right) + \left[- m_{Ar,Ne} \ln\left(r \frac{^4He}{CO_2}\right)_o + \ln\left(\frac{^{40}Ar}{CO_2}\right)_o \right] \quad (5)$$

It is important to note that with two radiogenic pairs—$^{21}Ne^*/^4He$ and $^4He/^{40}Ar^*$—it is possible to "fix" the degassing trajectory using one isotope pair (for example, $^{21}Ne^*/^4He$) then to investigate fractionation *prior* to magmatic degassing using the second pair ($^4He/^{40}Ar^*$). While this scheme can correct for magmatic degassing, there are two potential problems extrapolating to the modeled $^{21}Ne/^4He$ production ratio of 4.5×10^{-8}:

1. there are uncertainties in the actual $^{21}Ne/^4He$ ratio that is produced in the mantle; and
2. He and Ne may fractionate from each other before magmatic degassing, such that the "initial" magmatic $^{21}Ne/^4He$ ratio may not be the same as the ratio produced in the mantle.

Irrespective of the true $^{21}Ne/^4He$ production ratio, correcting to a *consistent* $^{21}Ne/^4He$ ratio allows comparison of "initial" $^4He/^{40}Ar$ ratios between samples that have undergone variable degrees of degassing. Therefore, uncertainties in the theoretical $^{21}Ne/^4He$ production ratio do not preclude comparison of "initial" $^4He/^{40}Ar$ ratios, although these uncertainties obviously will result in erroneous estimates of the absolute "initial" $^4He/^{40}Ar$ ratio.

The second problem, He/Ne fractionation before degassing, is more serious. If it can be demonstrated that He fractionates from Ar before magmatic degassing (for example, if "initial" $^4He/^{40}Ar$ ratios are inconsistent with production ratios), then it is probable that He has also fractionated from Ne and the central assumption to performing these corrections—that the initial magma has $^{21}Ne/^4He = 4.5 \times 10^{-8}$—is not valid. As a result, correcting for magmatic degassing using the above method will provide the *minimum* possible "initial" $^4He/^{40}Ar^*$ ratio. The discrepancy between the calculated and true "initial" $^4He/^{40}Ar$ ratios will increase with increasing deviation from the production ratio (i.e., the more anomalous the "initial" $^4He/^{40}Ar$ is, the more this method will underestimate the actual "initial" value). In theory, it is possible to use $^{136}Xe^*/^4He$ ratio to constrain fractionation before magmatic degassing (^{136}Xe is also produced by U-series decay). However, these measurements are not trivial to perform and it is difficult to imagine that sufficient quantitative information could be obtained.

2.5. Modeled Degassing of Basalts

2.5.1 Solubilities

The solubilities of CO_2 and the noble gases in silicate melts have been determined experimentally (e.g., Blank and Brooker, 1994; Carroll and Webster, 1994). Note that noble gas solubilities are not determined in the same experiments as CO_2 solubilities. These experiments have shown that solubilities increase Ar<Ne<CO_2<He in basaltic melts of tholeiitic composition. As a result, He/CO_2 will increase as a basaltic melt loses its volatiles whereas Ne/CO_2 and Ar/CO_2 will both decrease with progressive gas loss.

Previous work has shown that CO_2 dissolves as a CO_3^{2-} ion in a melt, whereas the noble gases dissolve as neutral species. As a result, CO_2 solubilities increase linearly with pressure (over the range of likely MORB magmas), and CO_2 solubility at a given pressure (S_{CO2}) is related to the basalt chemistry, particularly those elements that affect the molecular structure of the basalt such as Al_2O_3 or the alkalis (Dixon, 1997). Empirical relationships between K_{CO2} (Henry's law constant) and the basalt composition have been determined (Dixon, 1997), allowing CO_2 solubilities to be calculated for a given composition at a given pressure.

Noble gases, on the other hand, dissolve as neutral species in interstitial "solubility sites" in the melt (Carroll and Stolper, 1993; Carroll and Webster, 1994). Empirical relationships developed by Carroll and co-workers relate noble gas solubility to ionic porosity, a measure of interstitial site availability. However, silicate melts are compressible, and ionic porosity reduces with pressure. As a result, Henry's law constants for the noble

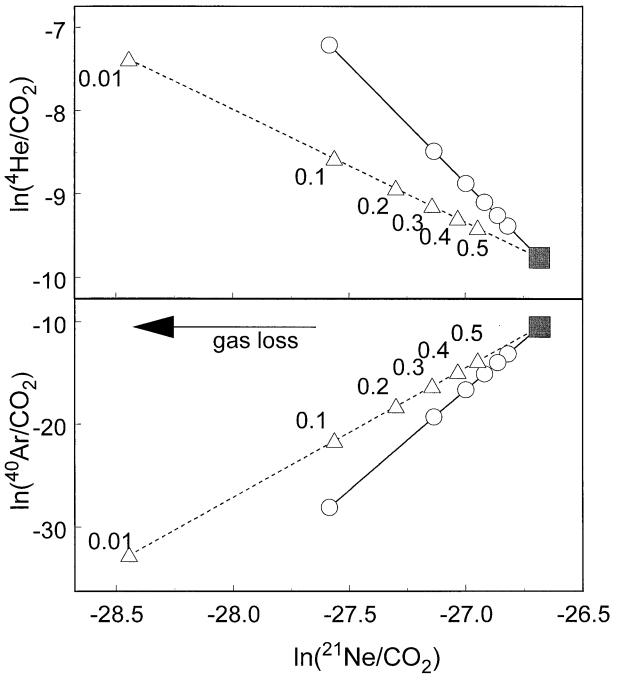

Fig. 2. Predicted volatile compositions in the melt remaining after Rayleigh distillation of a MORB-like magma. Starting compositions (gray box) assume $^{21}Ne/^{4}He$ and $^{4}He/^{40}Ar$ of 4.5×10^{-8} and 2, respectively. Relative noble gas:CO_2 solubilities are dependent on pressure as illustrated in Figure 1, resulting in a pressure dependence on the volatile compositions. Triangles: gas loss at 3 kbar; circles: gas loss at 0.3 kbar. Numbers next to symbols indicate fraction, F, of CO_2 remaining (i.e., $(CO_2)/(CO_2)_0$). The starting $^{4}He/CO_2$ composition (5.7×10^{-5}) is a reasonable MORB mantle estimate (Marty and Jambon, 1987; Marty and Tolstikhin, 1998).

gases are predicted to reduce with pressure (Chamorro-Perez et al., 1998).

2.5.2 Melt Compositions

The reduction in suitable solubility sites with pressure results in decreasing α_{Ar,CO_2}, α_{He,CO_2} and $\alpha_{Ne,CO2}$ with pressure for a given composition melt (Fig. 1; Appendix). Therefore, during Rayleigh distillation of magmatic volatiles, He/CO_2 in the melt will increase, and will increase more rapidly during gas loss at high pressure in comparison to gas loss at low pressure. The predicted trends for Rayleigh degassing of a melt at two representative pressures that span the likely range of MORB magma degassing are illustrated in Figure 2. Note that while the model predicts significant changes in the relative noble gas:CO_2 solubilities, a change in sign is not predicted; He is never less soluble than CO_2, nor are Ne or Ar more soluble.

Degassing occurs over a range in pressures (giving rise to different sized vesicles, for example, Burnard, 1999). As a result, early degassing from the magma could result in volatile compositions along or near (for example) the 3 kbar trajectory in Figure 2; as the magma decompresses, the volatile compositions will fall off the high pressure degassing trajectory and curve towards lower pressure trajectories. The effect of different degassing rates as a function of pressure is shown Figure 3. Increasing the fraction volatiles lost for a given decompression results in greater fractionation. However, it is difficult to quantitatively model the rate of degassing during decompression as this is dependent on poorly constrained initial volatile concentrations in the melt. The models presented here are necessarily simplistic.

2.5.3 Vesicle Compositions

While the volatiles remaining in the melt follow the trajectories outlined above, the majority of volatiles in a basaltic glass are usually trapped in vesicles rather than glass. He, Ne, Ar, and CO_2 will fractionate during vesicle formation. Jambon et al. (1986) showed that:

$$\frac{C_i^{ves}}{C_j^{ves}} = \frac{C_i^{tot}}{C_j^{tot}} \frac{\left(V^* + \rho S_j \frac{T_c}{T_o}\right)}{\left(V^* + \rho S_i \frac{T_c}{T_o}\right)}$$

Where superscripts "*ves*" and "*tot*" refer to the concentrations in vesicles and melt, respectively, V^* is the vesicularity, ρ is the density, and T_c, T_o are the closure temperature ($\approx$ 1000 K) and standard temperature ($=$ 273 K), respectively. Therefore, it is likely that the noble gas:CO_2 ratios dissolved in a basaltic *melt* will evolve along a specific trajectory depending on:

1. the initial compositions
2. the relative solubilities; and
3. the fraction of gas lost from the system

The noble gas:CO_2 ratio of a particular *vesicle* on the other hand will depend on:

1. the composition of the magma at the time the vesicle formed (in turn dependent on the degassing history of the magma)
2. the relative solubilities; and
3. the vesicularity at that episode of vesiculation

This is illustrated graphically in Figure 4. In general, fractionation resulting from vesicle—melt partitioning is minor in comparison to that resulting from Rayleigh distillation. High ($>$1%) vesicularities result in insignificant fractionation between vesicle and melt, whereas vesicularities $\approx$0.5% result in elevated heavy/light noble gas abundance ratios in the vesicles relative to the magma (Fig. 4). If vesicularity is constant over the history of the magma, then vesicle compositions will lie on a trajectory parallel to the composition of the melt. However, if vesicularity varies (for example, vesicularity may well decrease with time due to lower degrees of overpressure required for nucleation), then the vesicle compositions will lie on a line that will have a slope different from that of the melt.

Irrespective of vesicle-melt fractionation and polybaric degassing, the fractionating volatile compositions will trend toward the composition of the first vesicles to be nucleated Therefore, it is possible to extrapolate any fractionation trend to the composition of the first vesicles to be nucleated. The composition of the first vesicles will be similar to "initial" melt compositions provided the fractionation between the first vesicles to be nucleated and the melt is small. Fractionation between vesicles and melt is unlikely to create significant errors in estimating "initial" noble gas relative abundances provided *the first vesicles did not form at low ($<$0.5%) vesicularities.*

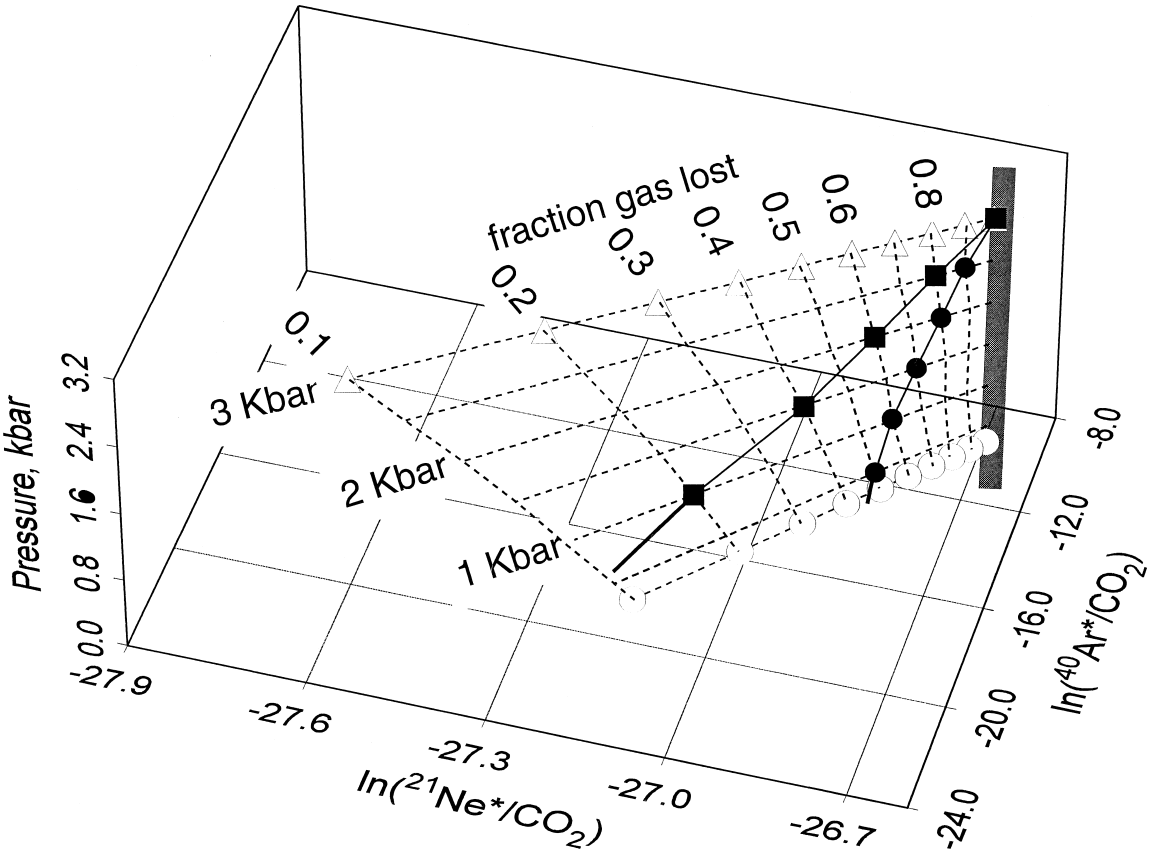

Fig. 3. Pressure dependent volatile fractionation (essentially a 3D version of the lower panel of Fig. 2 with pressure as the additional axis). Initial compositions (gray box) are as for Figure 2. Horizontal dashed lines are predicted trajectories for isobaric degassing over a range of pressures between 0.3 and 3 Kbar; open symbols show compositions for isobaric degassing at successive 10% gas loss intervals (as for Fig. 2). More probable polybaric degassing (solid lines and symbols) results in trajectories on the curved plane defined by the isobaric trajectories. A melt that starts degassing at 3 Kbar then loses 10% of its gas for each 0.5 Kbar decompression will follow the trend given by the filled circles. A more volatile - rich melt that had the same starting Ne-Ar-CO_2 composition would lose its volatiles more rapidly and lie on a different degassing trend. For example, the composition of volatiles in a melt that loses 20% of its volatiles for each 0.5 Kbar decompression is shown by the solid squares.

The vesicularity of the first episode of vesiculation is difficult to constrain, but is likely to be high—higher than any other episode—due to supersaturation resulting from lack of suitable nucleation sites.

2.6. Sequential Crushing and Unraveling Volatile Fractionation

Vesicles grow during ascent of a magma, primarily as a result of decompression (Proussevitch et al., 1993; Sahagian and Proussevitch, 1992; Sparks, 1978; Toramaru, 1989).Vesicles formed early in the system—at high pressure—will be larger than later vesicles, and the vesicles record a volatile "stratigraphy." Burnard (1999) showed that volatile compositions vary between vesicles, and that extracting gases from different sized vesicles provides a method of probing the volatile "stratigraphy."

Degassing trajectories vary from sample to sample (Burnard, 1999), depending on the "initial" volatile composition (i.e., that before degassing commenced), the relative noble gas and CO_2 solubilities (in turn dependent on the decompression rate and melt composition) and on the extent of vesiculation at each stage of degassing. Step crushing of basaltic glass will release volatiles from vesicles of different sizes—and therefore different stages in the volatile evolution—and can be used to determine the volatile trajectory of each particular sample.

Provided the volatile compositions of multiple analyses of a particular basalt may lie on a well defined trajectory, it is possible to extrapolate these back to the "initial" magmatic composition: Figure 4 demonstrates that, despite their subsequent complexities, volatile trajectories originate at the composition of the earliest vesicles in that magma. Contributions to ^{4}He, ^{21}Ne, and ^{40}Ar may also result from crustal contamination or posteruptive ingrowth, particularly in highly degassed magmas. However, it should be possible to asses significant non-

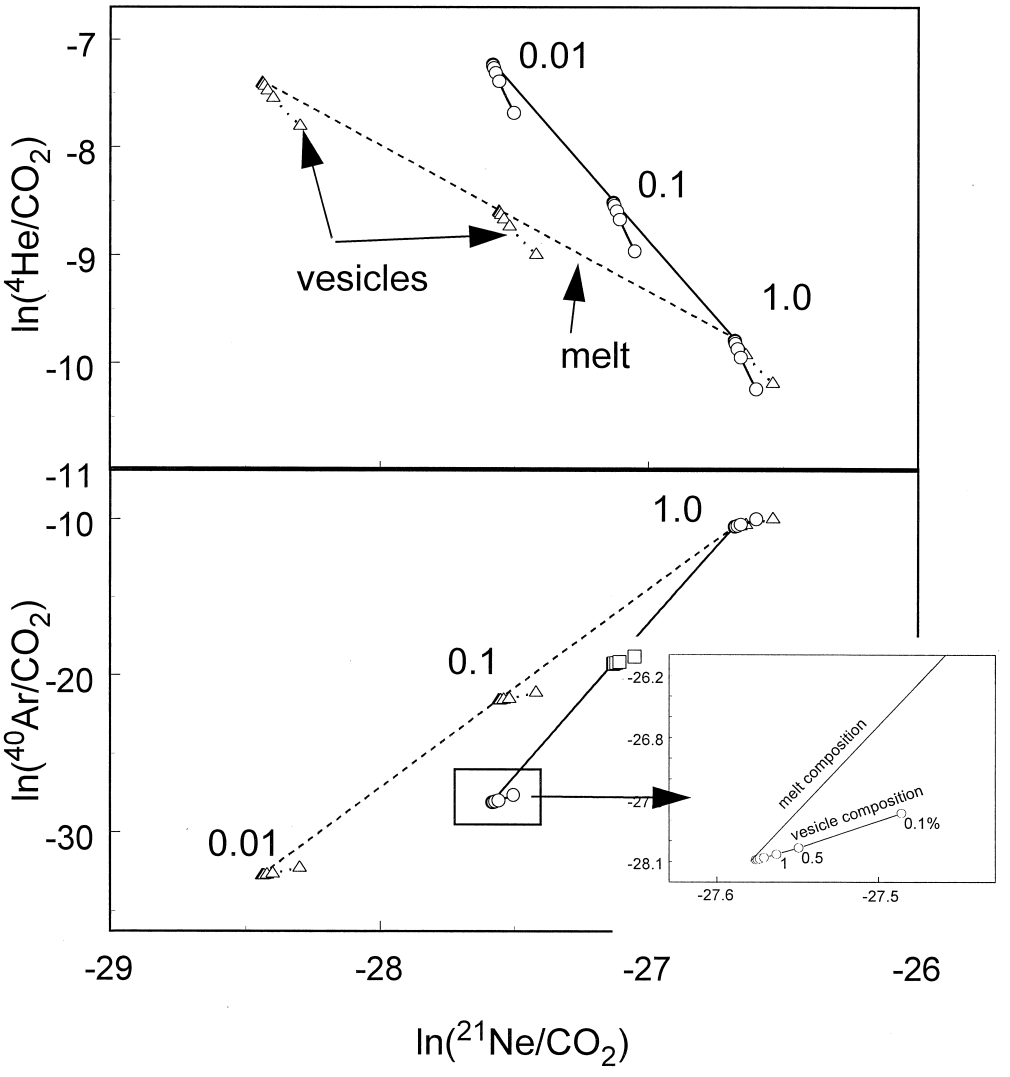

Fig. 4. As for Figure 2 but with the vesicle compositions superimposed on residual melt compositions (isobaric fractionation shown for simplicity). Symbols as for Figure 2, but shown for vesicle compositions that nucleated with vesicularities between 5% (which are indistinguishable from the melt composition) and 0.1% (most fractionated from melt composition). Vesiculation at three episodes of magmatic volatile evolution (F = 1, 0.1, and 0.01) have been illustrated. Therefore, the first vesicle to nucleate—with no gas lost from the magma—will have a composition on the vesicle evolution line at F = 1.0; the precise composition of that vesicle will depend on the vesicularity at that time. Assuming the magma continues to lose volatiles, a vesicle that formed later in the magmatic history (for example at F = 0.1) will have a composition on the vesicle evolution line at F = 0.1, the actual vesicle composition depending on vesicularity when it formed. Inset: detail of fractionation between vesicle and melt at vesicularities between 0.1 and 5%.

mantle derived contributions (in MORBs, at least) through the radiogenic/non-radiogenic noble gas isotope ratios ($^4He/^3He$, $^{21}Ne/^{22}Ne$, etc.).

The methods outlined above can be used to determine the volatile composition before degassing, and thereby investigate relative noble gas fractionation before magmatic fractionation. This is illustrated below using a basaltic glass sample previously analyzed by laser and known to have trapped variable composition volatiles (Burnard, 1999)

2.6.1 AMK3376

Coarse (>5 mm) chunks of clean basalt glass were sequentially crushed and analyzed for He, Ne, Ar, and CO_2 following the technique of Harrison et al. (1999). The results are given in Table 1. The He, Ne, and Ar isotope systematics are consistent with other noble gas studies of MORB glasses. He/Ar generally increases during crushing such that later crush steps have higher He/Ar (Table 1; Fig. 5), consistent with sampling smaller vesicles that have trapped more fractionated volatiles in later crush steps. The correlations (least squares fit) to the AMK3376 crushing steps that have detectable $^{21}Ne^*$ are (Fig. 6):

$$\ln(^4He/CO_2) = -0.32\ [\ln(^{21}Ne^*/CO_2)] - 18.7$$

$$\ln(^{40}Ar/CO_2) = 0.20\ [\ln(^{21}Ne^*/CO_2)] - 6.3$$

Substituting the above intercepts into Eqn. 4 and 5, the “initial”

Table 1. He, Ne and Ar released by stepped crushing of mid-Atlantic Ridge glass AMK3376.

Step	^{4}He, μcc STP	^{20}Ne, ncc STP	^{40}Ar, μcc STP	Total volatiles, mcc STP
CR1	0.328 ± 0.002	0.017 ± 0.001	0.053 ± 0.002	n.d.
CR2	2.34 ± 0.02	0.023 ± 0.001	0.31 ± 0.01	43 ± 5
CR3	3.35 ± 0.02	0.046 ± 0.002	0.47 ± 0.02	61 ± 7
CR4	4.96 ± 0.03	0.050 ± 0.002	0.70 ± 0.02	89 ± 10
CR5	1.4 ± 0.1	0.0304 ± 0.0003	0.127 ± 0.004	23 ± 3
CR6	6.8 ± 0.6	0.862 ± 0.008	0.89 ± 0.03	109 ± 13
CR7	2.4 ± 0.2	0.141 ± 0.002	0.34 ± 0.01	31 ± 4
CR8	0.41 ± 0.04	0.0227 ± 0.0002	0.038 ± 0.001	5 ± 1
CR9	0.19 ± 0.02	0.051 ± 0.001	0.056 ± 0.002	9 ± 1
Tot	22.2 ± 0.7	1.244 ± 0.008	2.99 ± 0.05	369 ± 19

Step	^{20}Ne/^{22}Ne	^{21}Ne/^{22}Ne	^{40}Ar/^{36}Ar	^{21}Ne* pcc STP
CR1	8.5 ± 0.8	0.036 ± 0.009	609 ± 6	
CR2	b.d.	b.d.[a]	13884 ± 508	
CR3	11.8 ± 1.1	0.043 ± 0.004	8617 ± 388	0.036 ± 0.006
CR4	12.8 ± 1.2	0.060 ± 0.004	18187 ± 3842	0.08±0.01
CR5	11.4 ± 1.1	b.d.[a]	5605 ± 135	
CR6	10.6 ± 1.2	0.0280 ± 0.0004	1105 ± 30	
CR7	10.0 ± 1.0	0.028 ± 0.001	646 ± 2	0.008 ± 0.001
CR8	10.0 ± 0.9	0.041 ± 0.004	3804 ± 309	0.0020 ± 0.0003
CR9	9.0 ± 0.9	0.030 ± 0.002	2641 ± 68	

^{4}He/CO_2 and $^{40}Ar^*/CO_2$ ratios in sample AMK3376 were $(42 \pm 3) \times 10^{-6}$ and $(9 \pm 2.0) \times 10^{-6}$, respectively. The ^{4}He/$^{40}Ar^*$ *before any degassing* was 4.7 ± 1.6 (assuming a mantle ^{20}Ne/^{22}Ne ratio of 13.8). Over 50% of the original volatiles were lost through magmatic degassing and the "initial" ^{4}He/CO_2 ratio of this sample ($\equiv C/^3He = 1.5 \times 10^9$) is similar to previous estimates of ^{4}He/CO_2 in the MORB source region (Marty and Jambon, 1987; Marty and Zimmerman, 1999).

The "initial" estimates by sequential crushing assume the ^{21}Ne/^{4}He production ratio of the mantle is 4.5×10^{-8} and that Rayleigh–type gas loss from the magma was responsible for the range in volatile compositions (i.e., diffusive losses and fractionation during vesiculation were minor). Even if both these assumptions are correct, it is important to appreciate it is still not possible to estimate the *actual* ^{4}He/$^{40}Ar^*$ of the primary magma: the "initial" ^{4}He/^{40}Ar (4.7 ± 1.6) appears to be higher than the likely production ratio in the mantle source region (1.6 – 3) at the 1 σ level. He was likely fractionated from Ar before degassing, although further data are required before the significance of this number can be determined. The same process that fractionated He from Ar likely fractionated ^{21}Ne from ^{4}He, therefore the assumption that the "initial" $^{21}Ne^*/^4He = 4.5 \times 10^{-8}$ cannot be correct; it appears that light noble gases have been preferentially incorporated into the magma, therefore the $^{21}Ne^*/^4$He initial ratio was probably lower than the production ratio. As a result, the "initial" ^{4}He/$^{40}Ar^*$ estimates using this method *are minimum estimates* to the true ^{4}He/^{40}Ar before degassing. However, the system is comparatively insensitive to discrepancies in "initial" $^{21}Ne^*/^4$He; e.g., if the "initial" $^{21}Ne^*/^4$He of the real system was half the production ratio (2.3×10^{-8})—in an extreme situation—then correcting the volatile trajectory to $^{21}Ne^*/^4He = 4.5 \times 10^{-8}$ would underestimate the true initial ^{4}He/$^{40}Ar^*$ by only 20%.

While it is not possible to obtain a precise estimate of the true initial ^{4}He/$^{40}Ar^*$ ratio, the "initial" ^{4}He/$^{40}Ar^*$ ratio of the undegassed parent melt to AMK3376 was clearly higher than plausible mantle production. Further data are required before the mechanism producing this fractionation can be determined; however, this example successfully demonstrates that it is possible to estimate ^{4}He/$^{40}Ar^*$ ratios before magmatic degassing.

This same sample was analyzed by laser decrepitation (Burnard, 1999), where correlated He-Ar-CO_2 compositions in different sized vesicles were used to extrapolate to "initial" ^{4}He/

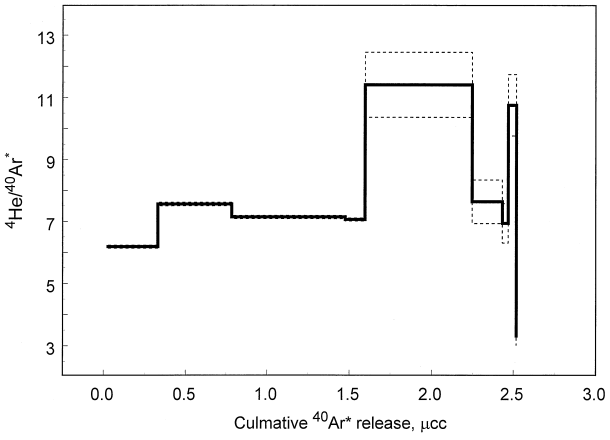

Fig. 5. ^{4}He/$^{40}Ar^*$ during stepped crushing. With the exception of two low gas release steps near the end of crushing, ^{4}He/$^{40}Ar^*$ generally increases with progressive crushing such that the lowest ^{4}He/$^{40}Ar^*$ ratios—the least fractionated volatiles—are released in the first few steps. This is consistent with the largest vesicles contributing most gas in the earliest crush steps. The lack of a smooth progression in ^{4}He/$^{40}Ar^*$ likely results from rupturing a small but variable number of comparatively large vesicles towards the end of crushing because the crushing apparatus does not crush to a uniform grainsize at each step.

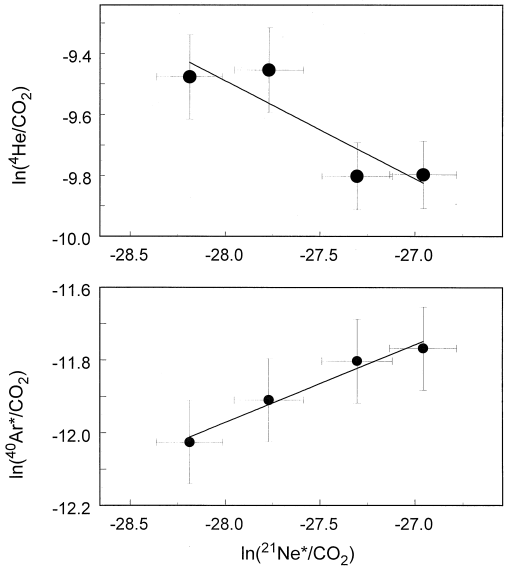

Fig. 6. He/CO_2 (top) and $^{40}Ar^*/CO_2$ (bottom) vs. $^{21}Ne^*/CO_2$ for individual AMK3376 crushing steps. These correlated variations in noble gas concentration in the volatile phase ($\equiv$ He, Ne, or Ar/CO_2) are thought to result from releasing the volatiles from progressively smaller vesicles as crushing progresses. The earliest formed vesicles—as sampled by the first crush—preserve the lowest Ar/CO_2 and Ne/CO_2 but the highest He/CO_2, consistent with volatile fractionation dominated by solubility determined processes. See text for meaning of slope and intercept.

CO_2 and $^{40}Ar^*/CO_2$ ratios. $^{40}Ar/CO_2$ ratios are significantly higher using the laser technique ($(9.7 - 12.4) \times 10^{-5}$). Some of the discrepancy is due to the fact that "initial" $^4He/^{40}Ar$ ratios were assumed to be at the production ratio for the earlier study, whereas this work shows that the "initial" $^4He/^{40}Ar$ ratio was significantly higher than production. Adjusting the "initial" estimates of the laser decrepitation study to $(^4He/^{40}Ar)_o = 4.7 \pm 1.6$ results in $(^4He/CO_2)_o$ and $(^{40}Ar/CO_2)_o$ in the range $(90 - 140) \times 10^{-6}$ and $(22 - 31) \times 10^{-6}$, respectively; nearly a factor of two higher than the estimates by crushing the same sample. Analytical artefacts are unlikely to cause this discrepancy as the laser technique tends to over estimate noble gas/CO_2 ratios (see discussion in Burnard, 1999). It is likely that the discrepancy is due to the small vesicles analyzed by the laser study (the technique is limited to vesicles <200 μm diameter). Small, late formed vesicles are more prone to magma—vesicle fractionation and require a larger extrapolation to the initial compositions than larger, early formed vesicles.

SUMMARY

Small vesicles trap more fractionated magmatic volatiles than early formed, large vesicles. Sequential crushing—which releases gas from progressively smaller vesicles—can be used to determine the trajectory of magmatic volatile evolution. Basaltic glasses are not likely to trap volatiles of a single composition, rather the fact that there is a range in vesicle sizes implies that a range in vesicle compositions should also be trapped. Sequential crushing releases gases from progressively smaller vesicles, providing a means of estimating the trajectory of compositions resulting from volatile fractionation during magma ascent. This is illustrated by sequential crushing of a glass from the mid Atlantic ridge; eight crushing steps had $^4He/^{40}Ar^*$ ratios in the range 6.2 to 11.4, with higher $^4He/^{40}Ar^*$ ratios in later crushing steps, consistent with sampling more fractionated volatiles in later crushing steps.

Modeling noble gas concentrations in the volatile phase ($\equiv$ noble gas:CO_2 ratios) shows that sequential crushing has the potential to deconvolve the magmatic degassing history, provided vesicularities were not below 0.5% during early stages of vesiculation. Degassing trajectories can be extrapolated to the mantle $^{21}Ne^*/^4He$ ratio, similar to correcting for magmatic differentiation by assuming a mantle MgO content of 8%. It is appropriate to extrapolate to a constant mantle $^{21}Ne^*/^4He$ because production of both ^{21}Ne and ^4He in the mantle is determined by the U+Th abundance, resulting in a constant $^{21}Ne/^4He$ production ratio irrespective of chemistry or accumulation time. It is anticipated that this method for correcting for magmatic volatile fractionation will allow variations in mantle relative noble gas abundances and the effects of mantle melting on relative noble gas abundances to be investigated.

Acknowledgments—Many thanks to Mike Carroll for supplying the ionic porosities spreadsheet. Comments by Chris Ballentine, Dave Hilton, and an anonymous reviewer were highly constructive. This work was carried out while the author was funded by the Caltech Postdoctoral fellowships program.

Associate editor: D. E. Fisher

REFERENCES

Allègre C. J., Staudacher T., and Sarda P. (1986) Rare gas systematics: formation of the atmosphere, evolution and structure of the Earth's mantle. *Earth Planet. Sci. Lett.* **81,** 127–150.

Allègre C. J., Staudacher T., Sarda P., and Kurz M. D. (1983) Constraints on evolution of Earth's Mantle from rare gas systematics. *Nature* **303,** 762–766.

Anderson D. L. (1998) The helium paradoxes. *Proc. Nat. Acad. Sci., USA.* **95,** 4822–4827.

Ballentine C. J. (1997) Resolving the mantle He/Ne and crustal $^{21}Ne/^{22}Ne$ in well gases. *Earth Planet. Sci. Lett.* **152,** 233–249.

Blank J. G. and Brooker R. A. (1994) Experimental studies of carbon dioxide in silicate melts: solubility, speciation, and stable carbon isotope behaviour. In *Volatiles in Magmas*, Vol. 30 (ed. M. R. Carroll and J. R. Holloway), pp. 157–182. Mineralogical Society of America.

Burnard P. G. (1999) The bubble-by-bubble volatile evolution of two mid-ocean ridge basalts. *Earth Planet. Sci. Lett.* **174,** 199–211.

Burnard P. G., Farley K. A., and Turner G. (1998) Multiple fluid pulses in a Samoan harzburgite. *Chem. Geol.* **148,** 99–114.

Burnard P. G., Graham D. W., and Turner G. (1997) Vesicle-specific noble gas analyses of "popping rock": implications for primordial noble gases in the Earth. *Science* **276,** 568–571.

Carroll M. R. and Stolper E. M. (1993) Noble gas solubilities in silicate melts and glasses: new experimental results for argon and the relationship between solubility and ionic porosity. *Geochim. Cosmochim. Acta* **57,** 5039–5052.

Carroll M. R. and Webster J. D. (1994) Solubilities of sulfur, noble gases, nitrogen, chlorine and fluorine in magmas. In *Volatiles in Magmas* (eds. M. R. Carroll and J. R. Holloway), Vol. **30**, pp. 231–271. Mineralogical Society of America.

Chamorro-Perez E., Gillet P., Jambon A., Badro J., and McMillan P. (1998) Low argon solubility in silicate melts at high pressures. *Nature* **393,** 352–355.

Dixon J. E. (1997) Degassing of alkalic basalts. *American Mineralogist.* **82,** 368–378.

Drescher J., Kirsten T., and Schäfer K. (1998) The rare gas inventory

of the continental crust, recovered by the KTB Continental Deep Drilling Project. *Earth Planet. Sci. Lett.* **154,** 247–263.
Farley K. A., Natland J., and Craig H. (1992) Binary mixing of enriched and undegassed (primitive?) mantle components (He, Sr, Nd, Pb) in Samoan lavas. *Earth Planet. Sci. Lett.* **111,** 183–199.
Fisher D. E. (1975) Trapped helium and argon and the formation of the atmosphere by degassing. *Nature* **256,** 113–114.
Fisher D. E. (1997) Helium, argon, and xenon in crushed and melted MORB. *Geochim. Cosmochim. Acta* **61,** 3003–3012.
Graham D. W., Castillo P. R., Lupton J. E., and Batiza R. (1996) Correlated He and Sr isotope ratios in the South Atlantic near-ridge seamounts and implications for mantle dynamics. *Earth Planet. Sci. Lett.* **144,** 491–503.
Harrison D. W., Burnard P. G., and Turner G. (1999) Noble gas behavior and composition in the Mantle: Constraints from the Iceland Plume. *Earth Planet. Sci. Lett.* **171,** 199–207.
Hilton D. R., Hammerschmidt K., Loock G., and Friedrichsen H. (1993) Helium and argon isotope systematics of the central Lau Basin and Valu Fa Ridge; evidence of crust/mantle interactions in a back-arc basin. *Geochim. Cosmochim. Acta* **57,** 2819–2841.
Hilton D. R., McMurtry G. M., and Kreulen R. (1997) Evidence for extensive degassing of the Hawaiian mantle plume from helium-carbon relationships at Kilauea Volcano. *Geophysical Research Letters* **24,** 3065–3068.
Hiyagon H., Ozima M., Marty B., Zashu S., and Sakai H. (1992) Noble gases in submarine glasses from mid-oceanic ridges and Loihi Seamount; constraints on early history of the Earth. *Geochim. Cosmochim. Acta* **56,** 1301–1316.
Honda M. and Patterson D. B. (1999) Systematic elemental fractionation of mantle-derived helium, neon, and argon in mid-oceanic ridge glasses. *Geochim. Cosmochim. Acta* **63,** 2863–2874.
Jambon A. (1994) Earth degassing and large-scale geochemical cycling of volatile elements. In *Volatiles in Magmas* (eds. M. R. Carroll and J. R. Holloway), Vol. **30**, pp. 479–509. Mineralogical Society of America.
Jambon A., Weber H., and Braun O. (1986) Solubility of He, Ne, Ar, Kr and Xe in a basalt melt in the range 1250–1600°C. Geochemical implications. *Geochim. Cosmochim. Acta* **50,** 401–408.
Jambon A., Weber H. W., and Begeman F. (1985) Helium and argon from an Atlantic MORB glass: concentration, distribution and isotopic composition. *Earth Planet. Sci. Lett.* **73,** 255–267.
Jochum K. P., Hofmann A. W., Ito E., Seufert H. M., and White W. M. (1983) K, U, and Th in mid-ocean ridge basalt glasses and heat production, K/U and K/Rb in the mantle. *Nature* **306,** 431–436.
Kellogg L. H. and Wasserburg G. J. (1990) The role of plumes in mantle He fluxes. *Earth Planet. Sci. Lett.* **99,** 276–789.
Kennedy B. M., Hiyagon H., and Reynolds J. H. (1990) Crustal Neon: a striking uniformity. *Earth Planet. Sci. Lett.* **98,** 227–289.
Klein E. M. and Langmuir C. H. (1987) Global correlations of ocean ridge basalt chemistry with axial depth and crustal thickness. *J. Geophys. Res.* **92,** 8089–8115.
Kurz M. D. and Jenkins W. J. (1981) The distribution of helium in oceanic basalt glasses. *Earth Planet. Sci. Lett.* **53,** 41–54.
Lange R. A. and Carmichael I. S. E. (1987) Densities of Na2O-K2O-CaO-MgO-FeO-Fe2O3-AL2O3-TiO2-SiO2 liquids: New measurements and derived partial molar properties. *Geochim. Cosmochim. Acta* **51,** 2931–2946.
Marty B., Zashu S., and Ozima M. (1983) Two noble gas components in a Mid-Atlantic Ridge basalt. *Nature (London)* **302,** 238–240.
Marty B. and Ozima M. (1986) Noble gas distribution in oceanic basalt glass. *Geochim. Cosmochim. Acta* **50,** 1093–1097.
Marty B. and Jambon A. (1987) C/3He in volatile fluxes from the solid Earth: implications for carbon geodynamics. *Earth Planet. Sci. Lett.* **83,** 16–26.
Marty B. and Tolstikhin I. N. (1998) CO2 fluxes from mid-ocean ridges, arcs and plumes, Geochemical Earth Reference Model (GERM). *Chem. Geol.* **145,** 233–248.
Marty B. and Zimmerman L. (1999) Volatiles (He, C, N, Ar) in mid-ocean ridge basalts: Assessment of shallow level fractionation and characterization of source composition. *Geochim. Cosmochim. Acta* **63,** 3619–3633.
Matsuda J.-i. and Marty B. (1995) The 40Ar/36Ar ratio of the undepleted mantle; a reevaluation. *Geophys. Res. Lett.* **22,** 1937–1940.
Moore J. G. (1979) Vesicularity and CO2 in mid-ocean ridge basalt. *Nature* **282,** 250–253.
Moreira M., Kunz J., and Allègre C. (1998) Rare Gas Systematics in Popping Rock: Isotopic and Elemental Compositions in the Upper Mantle. *Science* **279,** 1178–1181.
Moreira M. and Sarda P. (2000) Noble gas constraints on degassing processes. *Earth Planet. Sci. Lett.* **176,** 375–386.
O'Nions R. K. and McKenzie D. (1995) Estimates of mantle thorium/uranium ratios from Th, U and Pb isotope abundances in basaltic melts. *Phil. Trans. R. Soc. Lond.* **A342**, 65–77.
O'Nions R. K. and Tolstikhin I. N. (1994) Behavior and residence times of lithophile elements and rare gas tracers in the upper mantle. *Earth Planet. Sci. Lett.* **124,** 131–138.
Ozima M. and Podosek F. A. (1983) *Noble Gas Geochemistry*. Cambridge University Press.
Porcelli D. and Wasserburg G. J. (1995) Mass transfer of helium, neon, argon and xenon through a steady - state upper mantle. *Geochim. Cosmochim. Acta* **59,** 4921–4937.
Proussevitch A. A., Sahagian D. L., and Anderson A. T. (1993) Dynamics of diffusive bubble growth in magmas: isothermal case. *J. Geophys. Res.* **98,** 22283–22307.
Sahagian D. L. and Proussevitch A. A. (1992) Bubbles in volcanic systems. *Nature* **359,** 485.
Sarda P., Staudacher T., and Allègre C. (1988) Neon isotopes in submarine basalts. *Earth Planet. Sci. Lett.* **91,** 73–88.
Shannon R. D. (1976) Revised effective ionic radii and systematic studies of interatomic distances in halides and chalcogenides. *Acta Crystallographa* **A32**, 751–767.
Sparks R. S. J. (1978) The dynamics of bubble formation and growth in magmas: a review and analysis. *J. Volcanol. Geotherm. Res.* **3,** 1–37.
Staudacher T., Sarda P., Richardson S. H., Allègre C. J., Sagna I., and Dimitriev L. V. (1989) Noble gases in basalt glasses from a Mid-Atlantic Ridge topographic high at 14 N: Geodynamic consequences. *Earth Planet. Sci. Lett.* **96,** 119–133.
Toramaru A. (1989) Vesiculation processes and bubble size distributions in ascending magmas with constant velocities. *J. Geophys. Res.* **94,** 17523–17542.
Trieloff M., Kunz J., Clague D. A., Harrison D., and Allègre C. J. (2000) The nature of pristine noble gases mantle plumes. *Science* **288,** 1036–1038.
Yatsevich I. and Honda M. (1997) Production of nucleogenic neon in the Earth from natural radioactive decay. *J. Geophys. Res.* **102,** 10291–10298.

APPENDIX: CALCULATION OF NOBLE GAS AND CO_2 SOLUBILITIES.

Noble gas solubilities were calculated using Carroll and Stolper (1993):

$$\ln[X_i] = m_i \mathrm{IP} + b_i$$

Where $[X_i]$ is the mole fraction dissolved noble gas, m and b are determined empirically (the values used here are: $m_{He} = 0.344$; $m_{Ne} = 0.61$; $m_{Ar} = 0.796$; $b_{He} = -29.72$; $b_{Ne} = -43.12$; $b_{Ar} = -53.35$) and IP is the ionic porosity:

$$\mathrm{IP} = (\Sigma X_i V_i - \Sigma X_i A_i)/\Sigma X_i V_i$$

where X_i is the oxide mole fraction, V_i and A_i are the partial molar volumes and oxide volumes, respectively.

The ionic porosity was assumed to decrease with pressure due to the pressure dependence of V_i. Partial molar volumes for the major oxides at any given pressure were calculated from partial molar volumes and isothermal compressibilities from Lange and Carmichael (1987) at 1400 K and ionic radii from Shannon (1976). Noble gas partial molar volumes are assumed to be independent of pressure in this model; while this is unlikely to be realistic, note that decreasing the noble gas partial molar volumes (as is likely at high pressure) will likely increase their solubilities. Therefore, the pressure dependence of the noble gas partial molar volumes will likely decrease the pressure dependence of the α values calculated here.